Nonconventional Hydrogen Bonding between Clusters of Gold and Hydrogen Fluoride

ARTICLE *in* THE JOURNAL OF PHYSICAL CHEMISTRY A · AUGUST 2005

Impact Factor: 2.69 · DOI: 10.1021/jp052460q · Source: PubMed

3 AUTHORS:

Eugene S Kryachko
University of Liège
139 PUBLICATIONS **2,031** CITATIONS
SEE PROFILE

Alfred Karpfen
University of Vienna
162 PUBLICATIONS **4,284** CITATIONS
SEE PROFILE

F. Remacle
University of Liège
185 PUBLICATIONS **3,532** CITATIONS
SEE PROFILE

Nonconventional Hydrogen Bonding between Clusters of Gold and Hydrogen Fluoride

E. S. Kryachko,*,†,‡,§ A. Karpfen,∥,⊥ and F. Remacle*,†,#

Department of Chemistry, Bat. B6c, University of Liège, Sart-Tilman, B-4000, Liège, Belgium, Bogoliubov Institute for Theoretical Physics, Kiev, 03143, Ukraine, and Institute for Theoretical Chemistry, University of Vienna, Währinger Strasse 17, A-1090 Vienna, Austria

Received: May 11, 2005; In Final Form: June 16, 2005

The bonding patterns between small neutral gold $Au_{3\le n\le 7}$ and hydrogen fluoride $(HF)_{1\le m\le 4}$ clusters are discussed using a high-level density functional approach. Two types of interactions, anchoring Au−F and F−H···Au, govern the complexation of these clusters. The F−H···Au interaction exhibits all the characteristics of nonconventional hydrogen bonding and plays a leading role in stabilizing the lowest-energy complexes. The anchor bonding mainly activates the conventional F−H···F hydrogen bonds within HF clusters and reinforces the nonconventional F−H···Au one. The strength of the F−H···Au bonding, formed between the terminal conventional proton donor group FH and an unanchored gold atom, depends on the coordination of the involved gold atom: the less it is coordinated, the stronger its nonconventional proton acceptor ability. The strongest F−H···Au bond is formed between a HF dimer and the singly coordinated gold atom of a T-shape Au_4 cluster and is accompanied by a very large red shift (1023 cm^{-1}) of the ν(F−H) stretch. Estimations of the energies of formation of the F−H···Au bonds for the entire series of the studied complexes are provided.

1. Introduction

Within the classical theory of hydrogen bonding (see refs 1−8 and ref 9 for current review and references therein), the atoms F, N, O, C, P, S, Cl, Se, Br, and I, having a lone pair of sp-electrons, act as proton acceptors in forming conventional hydrogen bonds. Some transition metals also show a propensity to behave similarly with conventional proton donors, thereby generating nonclassical or nonconventional hydrogen bonds.[10] We have recently demonstrated that the coinage-metal cluster, Au_3, acts alike with formamide and formic acid,[11a] and DNA bases.[11b] It forms weak nonconventional N−H···Au and O−H···Au hydrogen bonds, provided that another Au atom of the cluster is anchored to the nitrogen or oxygen atoms of these molecules. We refer to these hydrogen bonds as "anchor-assisted" in order to emphasize that the anchor bond plays the leading role in stabilizing the entire complex. It induces a substantial charge redistribution that makes the lone pair of $5d_{\pm 2}$- and 6s-electrons of the unanchored gold atom available for a conventional proton donor. The upper bound for the strength of these weak nonconventional H-bonds was estimated to be within 3−5 kcal·mol^{-1}.

In this paper, we discuss nonconventional H-bonding between $Au_{3\le n\le 7}$ gold clusters and typical, classical hydrogen-bonded systems, the hydrogen fluoride clusters $(HF)_{2\le m\le 4}$ (see ref 12 for current review and references therein). In doing so, our aim is 2-fold. First, it is demonstrated that the ability of small neutral gold clusters to act as proton acceptors is not limited to trimers but extends to somewhat larger neutral clusters, $Au_{4\le n\le 7}$, that too can form nonconventional F−H···Au hydrogen bonds with $(HF)_{2\le m\le 4}$. Using a high-level density functional approach, we provide below a clear evidence that the resulting F−H···Au bond shares all the common features of conventional hydrogen bonds and is stronger than the nonconventional H-bonds we investigated previously.[11]

Our second aim is to show that with the $(HF)_{2\le m\le 4}$ clusters, the hydrogen bonding interaction is the key factor that determines the stabilization of the complexes under study. This is unlike the case of the complexes between Au_3 and formamide, formic acid, and DNA bases, where the formation of the anchoring N−Au or O−Au is a necessary prerequisite for the nonconventional N−H···Au or O−H···Au bonding to take place.

The paper is organized as follows. The computational aspects are outlined in section 2. In section 3, we first discuss in subsection 3.1 the structure and energetics of the $Au_3-(HF)_{1\le m\le 4}$ complexes. We in particular emphasize how the mechanism for the stabilization of the $Au_3-(HF)_m$ complexes varies when more than one HF molecules interact with the gold trimer. In subsection 3.2, we discuss the effect of increasing the size of the Au cluster on the stability of the $Au_n-(HF)_2$ complexes. Concluding remarks and a summary of the results are provided in section 4.

2. Computational Methodology

All computations of the complexes $Au_{3\le n\le 7}-(HF)_{1\le m\le 4}$ were conducted using the GAUSSIAN 03 package of quantum chemical programs.[13] The Kohn−Sham self-consistent-field formalism was used in conjunction with the hybrid density functional B3LYP potential. The basis sets chosen are 6-311++G(2d,2p) (≡A) and aug-cc-pVTZ (≡B) for the hydrogen fluoride clusters (see ref 14 for current use of these basis sets in computations of the rings $(HF)_{1\le m\le 4}$) and the energy-consistent $19-5s^25p^65d^{10}6s^1$-valence-electron relativistic effective core potential (RECP) of Ermler, Christiansen and coworkers[15] for the gold atoms (for its recent application to gold

† University of Liège.
‡ Bogoliubov Institute for Theoretical Physics.
§ Fax: +32 (4) 366 3413. E-mail: eugene.kryachko@ulg.ac.be.
∥ University of Vienna.
⊥ Fax: +43 1 4277 9527. E-mail: alfred.karpfen@univie.ac.at.
Maître de Recherches, FNRS (Belgium). Fax: +32 (4) 366 3413. E-mail: fremacle@ulg.ac.be.

10.1021/jp052460q CCC: $30.25
Published on Web 07/21/2005

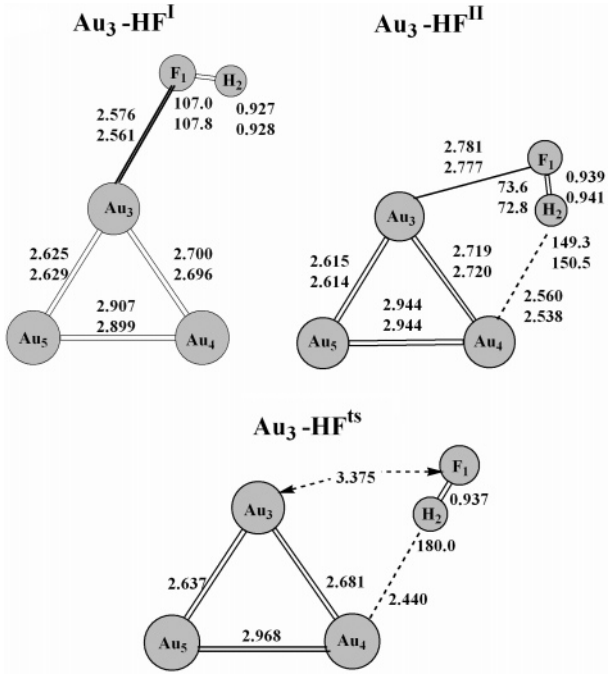

Figure 1. Lower-energy complexes of Au_3-HF obtained within the B3LYP/RECP(Au)∪A(H,F) (top entry) and B3LYP/RECP(Au)∪B(H,F) (lower entry) approaches. Some selected properties of these complexes relevant for a further discussion are collected in Table 1. The complex Au_3-HF^{I} is almost twice as polar (2.6−2.8 D) as the Au_3-HF^{II} one (1.4−1.5 D). The transition-state structure Au_3-HF^{ts} is identified within the B3LYP/RECP(Au)∪A(H,F) approach. The bond lengths are given in Å and bond angles in deg.

clusters see ref 16 and references therein). All geometrical optimizations were carried out with the keywords "tight" and "Int=UltraFine". The harmonic vibrational frequencies, zero-point vibrational energies (ZPVE), and enthalpies were also calculated. The reported binding energies are ZPVE-corrected.

Within the present computational approach, the triangular structure of Au_3 gold cluster is characterized by the electronic energy of −407.907290 hartree, ZPVE = 0.418 kcal·mol^{-1}, and the enthalpy equal to −407.900617 hartree. Its geometry is determined by $r(Au_1-Au_2) = r(Au_2-Au_3) = 2.654$ Å, $r(Au_1-Au_3) = 2.992$ Å, and the bond angle $\angle Au_1Au_2Au_3 = 68.6°$. The chain structure Au_3^{ch} is characterized by the electronic energy of −407.911124 hartree, ZPVE = 0.427 kcal·mol^{-1}, and the enthalpy equal to −407.904441 hartree. Its bond lengths $r(Au_1-Au_2) = r(Au_1-Au_3) = 2.619$ Å and the bond angle $\angle Au_2Au_1Au_3 = 115.2°$. The chain structure is the most stable conformer of Au_3 lying below the triangle structure by 2.4 kcal·mol^{-1}, after ZPVE (this value is however within a range of a so-called density functional margin equal approximately to 4 kcal·mol^{-1}; see ref 16 for the definition). Throughout the present work, Au_3 is identified with the triangular gold cluster. The B3LYP properties of the $(HF)_{1\le m\le 4}$ clusters are very similar to those early reported in refs 12 and 14 (see in particular Table 2 of ref 14a and also ref 17). The necessary and sufficient conditions that define conventional hydrogen bonds[1−9] (see also ref 18) were early summarized in ref 11a.

3. Nonconventional F−H···Au Hydrogen Bonding in $Au_3-(HF)_{1\le m\le 4}$ and $Au_{4\le n\le 7}-(HF)_2$

3.1. Potential Energy Surfaces of the $Au_3-(HF)_{1\le m\le 4}$ Interaction. The complex Au_3-HF has two nearly isoenergetic conformers, Au_3-HF^{I} and Au_3-HF^{II}, shown in Figure 1 (Au_3-HF^{II} is slightly lower by $\Delta E_b = 0.3$ kcal·mol^{-1}). The transition-state structure Au_3-HF^{ts}, also shown in Figure 1, links Au_3-HF^{I} to Au_3-HF^{II}. The corresponding barrier is only 0.1 kcal·mol^{-1} so that the HF molecule almost freely rotates between the two positions it occupies in Au_3-HF^{I} and Au_3-HF^{II}.

The complex Au_3-HF^{I} is mainly stabilized via a gold−halogen anchor bonding. The formation of the gold−halogen anchor bond is accompanied by an electron charge transfer from the F_1 atom to the Au_3 cluster that induces minor changes in the HF bond length (of ∼0.004−0.005 Å) and F−H stretch, ν(F−H) (of ∼−60 cm^{-1}) compared to the isolated HF molecule. On the other hand, the Au_4-H_2 contact, whose Au−H separation of 2.98 Å exceeds 2.86 Å, the sum of the van der Waals radii of Au and H, is very weak.

In contrast, the interaction between the unanchored gold atom Au_4 and the HF molecule, resulting in the $F_1-H_2\cdots Au_4$ bonding, is the main stabilization factor of the complex Au_3-HF^{II}. This is indicated by the two following geometrical features: (i) the anchor bond in Au_3-HF^{II} is much weaker than in Au_3-HF^{I} (viz., 2.78 Å vs 2.56−2.58 Å, respectively) and (ii) the Au_4-H_2 contact is much shorter, 2.54−2.56 Å vs 2.98 Å. It is even ∼0.02 Å shorter than the anchor bond in Au_3-HF^{I}. In addition, the formation of the $F_1-H_2\cdots Au_4$ bond in Au_3-HF^{II} induces significant changes in both interacting species. Within the HF molecule, the F_1-H_2 bond elongates by 0.017 Å, the corresponding $\nu(F_1-H_2)$ stretching vibrational mode downshifts by 370−379 cm^{-1} (its IR activity is enhanced by a factor of 5), and the proton nuclear magnetic resonance (^{1}H NMR) chemical shift $\delta\sigma_{iso}(H_2)$ of the bridging proton in the $F_1-H_2\cdots Au_4$ bond goes downfield by −2.6 ppm. This value is close to the value, $\delta\sigma_{iso}(H) = -2.8$ ppm, of the bridging proton in water dimer, which is the classical representative of hydrogen-bonded systems.[18c] These changes, affecting three different observables of the HF molecule, are induced by its interaction with a three-gold cluster. They are typical (see refs 1−9 and 11) of the nonconventional hydrogen bond $F_1-H_2\cdots Au_4$ that stabilizes the complex Au_3-HF^{II}. In this bond, the unanchored atom Au_4 of the gold trimer acts as a nonconventional proton acceptor with respect to the conventional F−H donor group.

In addition, the total potential energy surface (PES) of Au_3-HF also includes two conformers, $Au_3^{ch}-HF^{I}$ and $Au_3^{ch}-HF^{II}$, formed by the chain three-gold cluster, Au_3^{ch}, and the HF molecule (Figure 2). Their relevant properties are summarized in Table 1. In fact, they are slightly more stable (within 1.0−1.4 kcal·mol^{-1}) than those formed with the triangle gold cluster Au_3. Their formation, which solely occurs via the nonconventional F−H···Au hydrogen bonding, demonstrates that this type of bonding is able to stabilize the Au_3-HF complex without the presence of an anchoring Au−F bond.

As the number m of HF molecules involved in the complexation with a triangle gold cluster Au_3 increases from 1 to 4, the two basic interactions, viz., the anchoring Au−F and F−H··· Au bonding, cooperatively complement each other in stabilizing the most stable conformers, $Au_3-(HF)_{2\le m\le 4}^{I}$, displayed in Figures 3 ($m = 2$), 4 and 5 ($m = 3$), and 6 and 7 ($m = 4$). The $Au_3-(HF)_{2\le m\le 4}^{I}$ complexes can be structurally viewed as those where the Au−Au bonds simply play the part of one or two further HF molecules and can be therefore considered as resembling the structures of the $(HF)_{m+1}$ or $(HF)_{m+2}$ rings. In particular, the complexes $Au_3-(HF)_{3\le m\le 4}^{I}$ can be treated as originating either from an insertion of the triangle gold cluster in the ring $(HF)_{3\le m\le 4}$ or by substitution of a HF monomer or its dimer of the $(HF)_{m+1}$ or $(HF)_{m+2}$ rings, respectively, by Au_3. (by a direct analogy with ref 14). The complexes $Au_3^{ch}-$

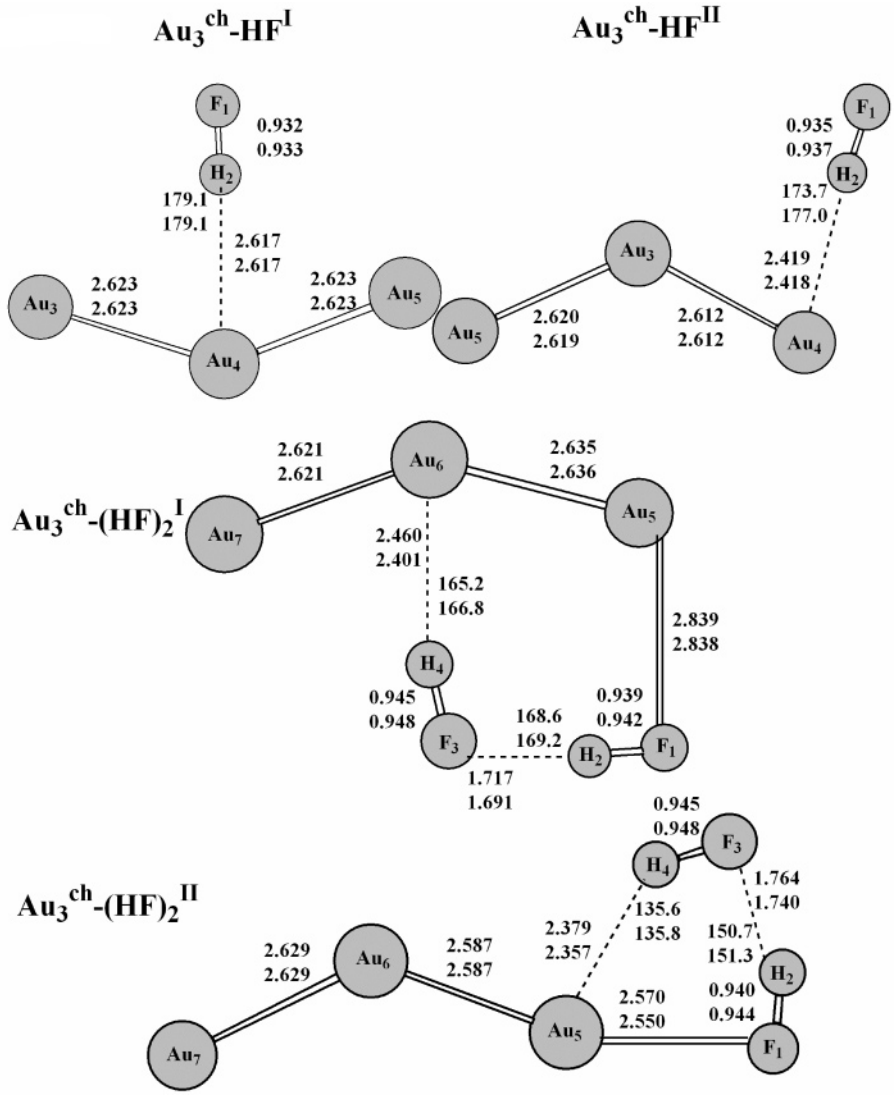

Figure 2. Lower-energy complexes of Au_3^{ch}−HF and Au_3^{ch}−$(HF)_2$ obtained within the B3LYP/RECP(Au)∪A(H,F) (top entry) and B3LYP/RECP-(Au)∪B(H,F) (lower entry) approaches. Some selected properties of these complexes relevant for a further discussion are collected in Table 1. The bond lengths are given in Å and bond angles in deg. In addition, the values of some bond angles of the structures Au_3^{ch}−$(HF)_2^I$: $\angle Au_5F_1H_2 = 88.6°^A$, $88.1°^B$, $\angle H_2F_3H_4 = 110.8°^A$, $110.1°^B$; and Au_3^{ch}−$(HF)_2^{II}$: $\angle Au_5F_1H_2 = 93.1°^A$, $92.8°^B$, $\angle H_2F_3H_4 = 94.5°^A$, $94.1°^B$.

$(HF)_{1\le m\le 2}$ are shown in Figure 2. The latter are, however, less stable, as follows from Table 1, and are therefore less important for the discussion below.

The anchor bond Au−F in the series Au_3−$(HF)_{2\le m\le 4}^I$ gradually contracts from 2.39 to 2.41 Å ($m = 2$) to 2.32−2.34 Å ($m = 4$) and hence strengthens as m increases (see Table 1). This is also true of the contact H···Au between the terminal hydrogen of the HF cluster and the unanchored gold atom (see Figures 1, 3−7) whose length decreases from 2.23 to 2.25 Å ($m = 2$) to 2.11−2.13 Å ($m = 4$). These two cooperative interactions lead to an increase of the binding energy (and of the absolute value of the enthalpy of formation, ΔH_f, defined in the legend of Table 1) of the planar complexes Au_3−$(HF)_{1\le m\le 3}^I$ when m increases from 1 to 3. Specifically, as m goes from 1 to 2, E_b abruptly rises by ca. 8 kcal·mol^{-1}. It is unlikely that such a large change in E_b arises from the hydrogen bonding within $(HF)_2$, whose binding energy itself amounts only 3−5 kcal·mol^{-1}.[12,17] Rather, the large increase in E_b can be explained in terms of a stronger character of both the anchor Au−F and the F−H···Au bonds in Au_3−$(HF)_2^I$ compared to Au_3−HF^I and Au_3−HF^{II}. When $m = 3$, the corresponding complex Au_3−$(HF)_3^I$ possesses the largest $E_b \approx 14$ kcal·mol^{-1}. The large binding energy of Au_3−$(HF)_3^I$ is partly a consequence of the rather low binding energy of the $(HF)_3$ ring, which results itself from the strongly nonlinear hydrogen bonds (see refs 12, 14, and 17). The local structure of the $(HF)_3$ moiety in Au_3−$(HF)_3^I$ is much closer to the structures of $(HF)_4$ or $(HF)_5$, oligomers with much stronger hydrogen bonds.

A binding of one additional HF molecule to Au_3−$(HF)_3^I$ results in the slightly puckered complex Au_3−$(HF)_4^I$ (Figure 6) whose binding energy is lowered to ∼10 kcal·mol^{-1} compared to that in Au_3−$(HF)_3^I$, despite the contraction by 0.06 Å of the Au−F anchor bond. In terms of $\Delta E_a = E_m - (E_{m-1} + E_1)$ where E_k is the total energy of the cluster $(HF)_k$, it is less stable than Au_3−$(HF)_3^I$. On the other hand, in terms of $\Delta E_b = (E_m - mE_1)/m$, Au_3−$(HF)_4^I$, which structurally resembles either $(HF)_5$ or $(HF)_6$, is not less stable than Au_3−$(HF)_3^I$: notice that the cyclic complex $(HF)_6$ is also slightly puckered, but its hydrogen bonds are still stronger than those in $(HF)_5$ (see ref 12).

We therefore demonstrate that the two types of interaction, that between the gold and fluorine atoms, and that between the unanchored atom of gold and the terminal HF molecule, determine the bonding patterns in the studied complexes Au_3−$(HF)_{2\le m\le 4}^I$. The gold−halogen anchoring activates the neighboring F−H···F conventional hydrogen bond and partially

TABLE 1: Selected Features of the Most Stable Complexes $Au_3-(HF)_{1\le m\le 4}$ and $Au_{4\le n\le 7}-(HF)_2$[a]

complex	E_b	ΔH_f	R(Au−F)	ν(F−H)
Au_3-HF^{I}	3.3	−3.1	2.576	4033 (147)
	3.1	−3.0	2.561	4009 (153)
Au_3-HF^{II}	3.6	−3.7	2.781	3727 (547)
	3.4	−3.6	2.777	3689 (558)
$Au_3^{ch}-HF^{I}$	2.5	−2.5		3873 (418)
	2.4	−2.3		3848 (408)
$Au_3^{ch}-HF^{II}$	2.1	−2.2		3779 (1056)
	2.1	−2.1		3757 (1034)
$Au_3-(HF)_2^{I}$	12.0	−12.4	2.414	3212 (1617), 3508 (767)
	12.1	−12.6	2.392	3149 (1537), 3433 (849)
$Au_3-(HF)_2^{II}$	4.9	−5.2	2.311	3504 (2245), 3880 (650)
	4.8	−4.6	2.298	3469 (2306), 3832 (664)
$Au_3^{ch}-(HF)_2^{I}$	5.8	−5.7	2.839	3602 (744), 3765 (212)
	5.7	−5.6	2.838	3536 (781), 3708 (218)
$Au_3^{ch}-(HF)_2^{II}$	5.2	−5.2	2.570	3611 (1051), 3752 (790)
	5.2	−5.2	2.550	3559 (986), 3694 (882)
$Au_3-(HF)_3^{I}$	13.6	−13.2	2.354	3018 (2539), 3294 (1755), 3451 (878)
	14.2	−13.9	2.331	2942 (2318), 3203 (2100), 3371 (859)
$Au_3-(HF)_3^{II}$	2.9	−1.9	2.584	3528 (921), 3741 (519), 3884 (632)
	2.8	−1.8	2.570	3455 (1012), 3687 (544), 3853 (624)
$Au_3^{ch}-(HF)_3$	7.9	−7.3	2.411	3325 (1264), 3480 (1027), 3601 (499)
	8.3	−7.8	2.381	3230 (1215), 3384 (1272), 3515 (478)
$Au_3-(HF)_4^{I}$	9.7	−8.9	2.343	2989 (2620), 3222 (2248), 3373 (1981), 3455 (208)
	10.1	−9.3	2.320	2912 (2299), 3122 (2842), 3286 (1981) ,3374 (172)
$Au_3-(HF)_4^{II}$	2.6	−1.4	2.625	3190 (1160) ,3431 (1176), 3545 (1659), 3670 (942)
	2.2	−1.2	2.624	3064 (1150), 3328 (1314), 3449 (1862), 3582 (997)
$Au_4-(HF)_2$	17.6	−17.9	2.350	3007 (1670), 3317 (663)
$Au_5-(HF)_2^{I}$	5.1	−4.5	2.627	3473 (1392), 3655 (484)
$Au_5-(HF)_2^{II}$	5.0	−4.4	2.577	3378 (1606), 3619 (597)
$Au_6-(HF)_2$	5.5	−5.0	2.619	3481 (1551), 3661 (536)
$Au_7-(HF)_2^{I}$	7.5	−6.9	2.532	3451 (1342) 3615 (463)
$Au_7-(HF)_2^{II}$	5.3	−4.6	2.600	3521 (1321), 3668 (604)
$Au_7-(HF)_2^{III}$	5.9	−5.4	2.615	3383 (1862), 3636 (619)
$Au_7-(HF)_2^{IV}$	4.4	−3.7	2.644	3555 (1374), 3693 (591)
$Au_7-(HF)_2^{V}$	3.9	−3.0	3.017	3591 (1261), 3783 (341)

[a] The binding energy E_b (including ZPVE, in kcal·mol^{-1}) and the enthalpy of formation, ΔH_f (kcal·mol^{-1}), are defined with respect to the infinitely separated monomers $Au_{3\le n\le 7}$ (Au_3^{ch}) and $(HF)_{1\le m\le 4}$. The length of the anchor Au−F bond is given in Å. Frequencies of the stretching vibrational modes ν(F−H) are given in cm^{-1} and reported with their IR activities (in parentheses, km·mol^{-1}). For $Au_3-(HF)_{1\le m\le 4}$, the upper entry corresponds to the basis A(H,F) and the lower corresponds to B(H,F). For $Au_{4\le n\le 7}-(HF)_2$, the total basis set is RECP(Au)∪B(H,F).

causes a charge redistribution within the three-gold and the hydrogen fluoride clusters (for example, the Mulliken charges in the complex $Au_3-(HF)_{2\le m\le 4}^{I}$ are changed as $\Delta q(F_1) = 0.067$, $\Delta q(H_2) = -0.014$, $\Delta q(F_3) = 0.040$, $\Delta q(H_4) = -0.101$, $\Delta q(Au_5) = 0.170$, and $\Delta q(Au_6) = 0.018$ $|e|$ relative to those in the monomers). On the other hand the intermolecular F−H···Au bonding governs the coordination of the terminal HF molecule to Au_3 cluster: the lone pair of the $5d_{\pm 2}$- and 6s-electrons of its unanchored atom of Au_3 being available for the conventional proton donor F−H group. Selected features of these intermolecular F−H···Au bonds in the complexes $Au_3-(HF)_{2\le m\le 4}^{I}$ are gathered in Table 2. Their comparison with the necessary and sufficient conditions, defining conventional hydrogen bonds (refs 1−9 and 11), leads to the conclusion that these bonds can be treated as nonconventional hydrogen bonds. The unusual, nonconventional character of the gold cluster as a proton acceptor in the latter hydrogen bonds makes them rather particular, in the following:

(a) The H-bond stretching vibrational mode ν_σ(F···Au) which is partly coupled to the Au−F anchor stretch in the computed IR spectra of the complexes $Au_3-(HF)_{2\le m\le 4}^{I}$ slightly increases with m: ν_σ(F···Au) = 138^{A}, 141^{B} cm^{-1} for $m = 2$ (the superscripts A and B indicate the basis sets used for the HF molecules), 142^{A}, 146^{B} cm^{-1} for $m = 3$, and 154^{A}, 156^{B} cm^{-1} for $m = 4$.

(b) It directly follows from Table 2 that all F−H···Au bonds in $Au_3-(HF)_{2\le m\le 4}^{I}$ are practically linear. For example, the bond angle $\angle F_7H_8Au_{10}$ in $Au_3-(HF)_4^{I} = 178.1°^{A}$ and $178.5°^{B}$.

(c) The F−H bond in the F−H···Au elongates relative to that of the monomer. As m increases from 2 to 4, there is a slow decline in the elongation from the maximum value of ca. 0.04 Å that corresponds to the F_3-H_4 bond in $Au_3-(HF)_2^{I}$ and that is almost twice larger than the elongation of the O−H bond of the O−H···Au nonconventional hydrogen bond is formed in the formic acid − Au_3 complex.[11a] Note also that this maximal elongation is larger than the elongation by 0.024−0.026 Å that the conventional H-bond $F_1-H_2\cdots F_3$ experiences in the same complex $Au_3-(HF)_2^{I}$.

(d) For all the complexes $Au_3-(HF)_{2\le m\le 4}^{I}$, the H-bond separation r(H···Au) is shorter than 2.86 Å, and therefore satisfies the van der Waals cutoff criterion. It narrows as m increases, viz., from 2.24 to 2.25 Å at $m = 2$ to 2.11−2.13 Å at $m = 4$ and is actually much shorter than the H-bond separation of the O−H···Au and N−H···Au H-bonds in the Au_3- formamide, formic acid, and DNA bases complexes.[11] In addition, the formation of the complexes $Au_3-(HF)_{2\le m\le 4}^{I}$ tends to strengthen the intramolecular conventional F−H···F hydrogen bonds within the HF clusters. This is clearly seen by comparing their bond lengths R(F−H) and r(H···F), and the bond angles ∠FHF with those of the cyclic $(HF)_m$ clusters. Regarding R(F−H), it is already noticed in (c) that R(F−H) of the F−H···F bonds increases under formation of $Au_3-(HF)_{2\le m\le 4}^{I}$. As follows from Figures 3, 4, and 6, the H-bond distances tend to shrink by 0.221−0.227 Å for $m = 2$, by 0.237−0.235 and 0.230−0.226 Å for $m = 3$, and by 0.073−0.075, 0.075−0.065, and 0.070−0.058 Å for $m = 4$. This obviously facilitates the electron

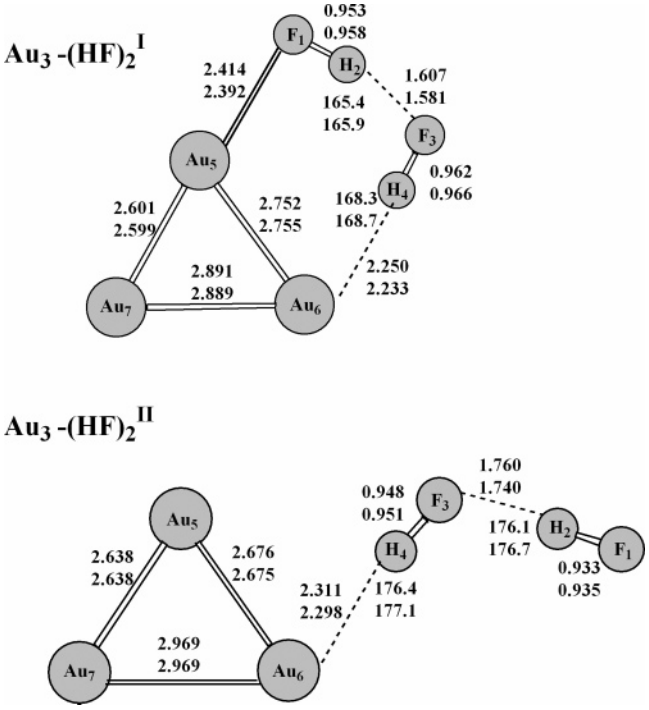

Figure 3. Low-energy portion of the PES of $Au_3-(HF)_2$ obtained within the B3LYP/RECP(Au)∪A(H,F) (top entry) and B3LYP/RECP-(Au)∪B(H,F) (lower entry) approaches. Some selected properties of these complexes relevant for a further discussion are collected in Table 1. The bond lengths are given in Å and bond angles in deg. In addition, the values of some bond angles of the structures **I**: $\angle Au_5F_1H_2 = 98.4°^A$, $98.0°^B$, $\angle H_2F_3H_4 = 106.1°^A$, $106.0°^B$; and **II**: $\angle H_2F_3H_4 = 115.5°^A$, $115.8°^B$.

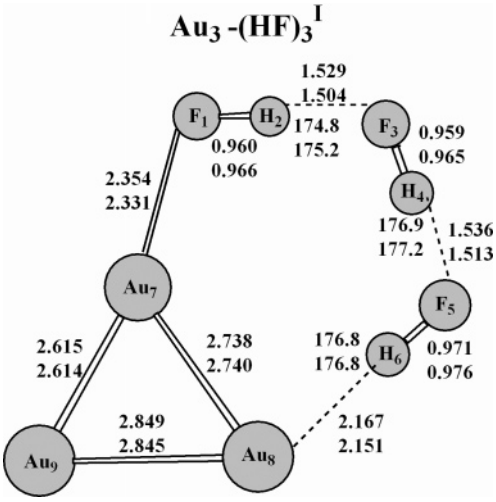

Figure 4. $Au_3-(HF)_3^I$ complex obtained within the B3LYP/RECP-(Au)∪A(H,F) (top entry) and B3LYP/RECP(Au)∪B(H,F) (lower entry) approaches. Its selected properties relevant for a further discussion are collected in Table 1. The bond lengths are given in Å and bond angles in deg. In addition, the values of some bond angles of $Au_3-(HF)_3^I$: $\angle Au_5F_1H_2 = 109.7°^A$, $109.5°^B$, $\angle H_2F_3H_4 = 114.1°^A$, $113.9°^B$, $\angle H_4F_5H_6 = 114.8°^A$, $114.8°^B$.

charge transfer between the proton donors and proton acceptors and activates the F−H···F bonds that are far from the anchor bond. It is also shown in Figures 3, 4, and 6 that, while the H-bond angle of the $F_1-H_2\cdots F_3$ bond in $Au_3-(HF)_2^I$ slightly decreases by 3.3−4.8° compared to that in the open hydrogen fluoride dimer, the related bond angles in the complexes $Au_3-(HF)_3^I$ and $Au_3-(HF)_4^I$ increase by 28−30° and 14−15°, with respect to those in the cyclic HF clusters $(HF)_3$ and $(HF)_4$. Therefore, the formation of the Au−F anchor and F−H···Au

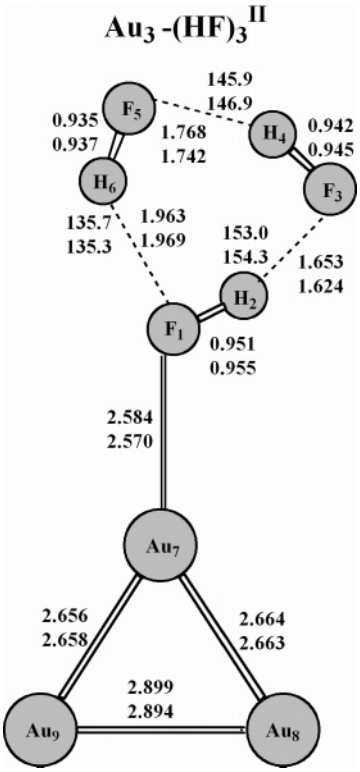

Figure 5. $Au_3-(HF)_3^{II}$ complex obtained within the B3LYP/RECP-(Au)∪A(H,F) (top entry) and B3LYP/RECP(Au)∪B(H,F) (lower entry) approaches. Its selected properties relevant for a further discussion are collected in Table 1. The bond lengths are given in Å and bond angles in deg. In addition, the values of some bond angles of the $Au_3-(HF)_3^{II}$: $\angle H_2F_3H_4 = 95.9°^A$, $95.4°^B$, $\angle H_4F_5H_6 = 99.1°^A$, $98.8°^B$, $\angle H_6F_1H_2 = 90.5°^A$, $89.4°^B$.

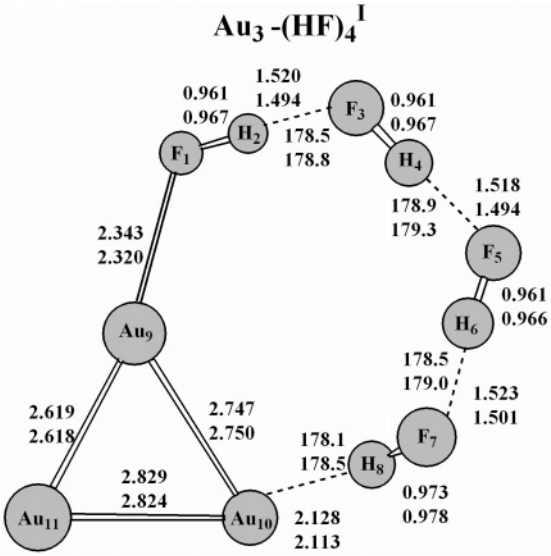

Figure 6. $Au_3-(HF)_4^I$ complex obtained within the B3LYP/RECP-(Au)∪A(H,F) (top entry) and B3LYP/RECP(Au)∪B(H,F) (lower entry) approaches. Its selected properties relevant for a further discussion are collected in Table 1. The bond lengths are given in Å and bond angles in deg. In addition, the values of some bond angles of $Au_3-(HF)_4^I$: $\angle Au_5F_1H_2 = 114.3°^A$, $114.4°^B$, $\angle H_2F_3H_4 = 117.9°^A$, $118.8°^B$, $\angle H_4F_5H_6 = 118.0°^A$, $118.3°^B$, $\angle H_6F_7H_8 = 115.6°^A$, $116.1°^B$.

bondings in $Au_3-(HF)_{2\le m\le 4}^I$ reinforces the bridged conventional F−H···F hydrogen bonds;

(e) The maximum red shift $\Delta\nu_{F-H\cdots Au}(F-H) = 844^A$, 881^B cm^{-1} is predicted for the complex $Au_3-(HF)_2^I$ whose F_3-H_4 bond maximally elongates. Its IR activity, A_{IR}, increases by a

TABLE 2: Selected Features of the Most Stable Complexes $Au_3-(HF)_{2\le m\le 4}$ Relevant to Prove Conditions ii−vi of the Conventional Hydrogen Bonds Listed in Ref 11A (See Also Refs 1−9)[a]

condition	$Au_3-(HF)_2$	$Au_3-(HF)_3$	$Au_3-(HF)_4$
ii	$\angle F_3H_4Au_6 = 168.3^{\circ A}, 168.7^{\circ B}$	$\angle F_5H_6Au_8 = 176.8^{\circ A}, 176.8^{\circ B}$	$\angle F_7H_8Au_{10} = 178.1^{\circ A}, 178.5^{\circ B}$
iii	$\Delta R(F_3-H_4) = 0.037^A, 0.038^B$ Å	$\Delta R(F_5-H_6) = 0.029^A, 0.031^B$ Å	$\Delta R(F_7-H_8) = 0.019^A, 0.017^B$ Å
iv	$r(H_4\cdots Au_6) = 2.250^A, 2.233^B$ Å	$r(H_6\cdots Au_8) = 2.167^A, 2.151^B$ Å	$r(H_8\cdots Au_{10}) = 2.128^A, 2.113^B$ Å
v	$-\Delta\nu(F_3-H_4) = 844^A, 881^B$ cm^{-1}	$-\Delta\nu(F_5-H_6)^b = 752^A, 776^B$ cm^{-1}	$-\Delta\nu(F_7-H_8)^b = 517^A, 490^B$ cm^{-1}
	$A_{IR}(F_3-H_4\cdots Au_6)/A_{IR}(F_3-H_4) = 12.2^A, 11.5^B$	$A_{IR}(F_5-H_6\cdots Au_8)/A_{IR}(F_5-H_6)^b = 3.4^A, 2.9^B$	$A_{IR}(F_7-H_8\cdots Au_{10})/A_{IR}(F_7-H_8)^b = 1.4^A, 1.1^B$
vi	$\delta\sigma_{iso}(H_4) = -4.4^A, -4.7^B$ ppm	$\delta\sigma_{iso}(H_6)^c = -1.6^A, -1.5^B$ ppm	$\delta\sigma_{iso}(H_8)^c = -0.1^A, +0.4^B$ ppm
	$\delta\sigma_{iso}(F_3) = -58.9^A, -62.2^B$ ppm	$\delta\sigma_{iso}(F_5)^c = -56.6^A, -57.3^B$ ppm	$\delta\sigma_{iso}(F_7)^c = -58.2^A, -57.3^B$ ppm
	$\delta\sigma_{iso}(Au_6) = 18.6^A, 18.5^B$ ppm	$\delta\sigma_{iso}(Au_8) = 20.7^A, 20.5^B$ ppm	$\delta\sigma_{iso}(Au_{10}) = 20.7^A, 20.5^B$ ppm
	$\delta\sigma_{an}(H_4) = 18.3^A, 18.8^B$ ppm	$\delta\sigma_{an}(H_6)^c = 16.7^A, 16.3^B$ ppm	$\delta\sigma_{an}(H_8)^c = 9.9^A, 9.0^B$ ppm
	$\delta\sigma_{an}(F_3) = 48.9^A, 49.8^B$ ppm	$\delta\sigma_{an}(F_5)^c = -78.5^A, -80.1^B$ ppm	$\delta\sigma_{an}(F_7)^c = 87.9^A, 91.3^B$ ppm
	$\delta\sigma_{an}(Au_6) = -39.5^A, -40.4^B$ ppm	$\delta\sigma_{an}(Au_8) = -41.2^A, -41.8^B$ ppm	$\delta\sigma_{an}(Au_{10}) = -40.9^A, -41.6^B$ ppm

[a] $\Delta\nu$(F−H) is a shift of the stretching mode ν(F−H) taken with respect to the corresponding monomer and A_{IR} stands for the IR activity. $\delta\sigma_{Iso}$ and $\delta\sigma_{an}$ (both in ppm) are taken with respect to the corresponding monomers. The two employed bases, A and B, for HF clusters are indicated by the corresponding superscripts. [b] Relative to the asymmetric degenerate vibrational modes of the cyclic complexes $(HF)_3$ and $(HF)_4$, respectively. [c] Relative to the NMR data of the cyclic complexes $(HF)_3$ and $(HF)_4$, respectively.

factor of about 12. It exceeds that in the formic acid−Au_3 complex[11a] by a factor of ca. 2. Since the corresponding clusters $(HF)_3$ and $(HF)_4$ are cyclic (C_{nh}-symmetric) and hence possess only degenerate F−H stretching vibrational modes which are IR-active (see ref 14), the comparison of the ν(F−H) and the ratio A_{IR}(F−H···Au)/A_{IR}(F−H) for the complexes $Au_3-(HF)_{3\le m\le 4}^I$ is unsatisfactory. There is, however, another way that consists of comparing the red shifts of the F−H···Au bond with those of the conventional F−H···F ones, within the same complex. The formation of the HF dimer causes a red shift of 150−160 cm^{-1} of the ν(F−H) stretch, along with an increase of its IR activity by a factor of 4. A bonding of this HF dimer to a three-gold cluster further downshifts the $\nu_{F-H\cdots F}$(F−H) stretch by 443^A, 472^B cm^{-1} and increases its IR activity by a factor of ca. 1.6. Compared to the HF monomer, the $\nu_{F-H\cdots F}$-(F−H) stretch in $Au_3-(HF)_2^I$ gains a total red shift of 632 cm^{-1} at most, whereas the $\Delta\nu_{F-H\cdots Au}$(F−H) shifts amounts to 38 (a red shift in the HF dimer) + 881 = 919 cm^{-1}. That is larger by 287 cm^{-1} compared to $\Delta\nu_{F-H\cdots F}$(F−H). Finally, the fact that the ratio of IR activities of the F−H stretches of the F−H···Au and F−H···F bonds is equal to 2.1 corroborates the stronger character of the former bond over the latter. Energetically speaking and taking into account that the ratio $\Delta\nu_{F-H\cdots Au}$(F−H)/$\nu_{F-H\cdots F}$(F−H) ≈ 1.45, one estimates the energy of formation of the F−H···Au bond as approximately equal to −7 to −4 kcal·mol^{-1}. It is worth also mentioning that the difference $\nu_{F-H\cdots Au}$(F−H) − $\nu_{F-H\cdots F}$(F−H) is equal to −276 cm^{-1} for $m = 3$ and −233 cm^{-1} for $m = 4$, and the corresponding ratios A_{IR}-($\nu_{F-H\cdots Au}$(F−H))/A_{IR}($\nu_{F-H\cdots F}$(F−H)) = 1.4 and 1.2;

(f) The NMR isotropic chemical shift $\delta\sigma_{iso}$(H) of the bridging proton in the F−H···Au bond in the studied complexes $Au_3-(HF)_{2\le m\le 4}^I$ is negative, as required if the hydrogen bond formation induces a deshielding of the bridging proton. $\delta\sigma_{iso}$-(H) amounts to -4.4^A, -4.7^B ppm for $m = 2$ (see Table 2). This shift nearly coincides with $\delta\sigma_{iso}(H_2) = -4.3^A, -4.8^B$ ppm of the bridging proton H_2 that belongs to the conventional hydrogen bond $F_1-H_2\cdots F_3$ and is larger in absolute value than $\delta\sigma_{iso}$(H) obtained for the formic acid−Au_3 complex.[11a] As in **(e)**, a comparison of the NMR chemical shifts of $Au_3-(HF)_{3\le m\le 4}^I$ with those of the cyclic clusters $(HF)_3$ and $(HF)_4$ is rather ill-defined. A more consistent procedure consists of comparing the former with the conventional F−H···F hydrogen bond within the same complex. We find that $\sigma_{iso}(H_6) - \sigma_{iso}(H_2) = 1.7$ ppm and $\sigma_{iso}(H_6) - \sigma_{iso}(H_4) = 1.9$ ppm for $m = 3$ and $\sigma_{iso}(H_8) - \sigma_{iso}(H_2) = 0.7$ ppm, $\sigma_{iso}(H_8) - \sigma_{iso}(H_4) = 1.2$ ppm, and $\sigma_{iso}(H_8) - \sigma_{iso}(H_6) = 1.1$ ppm for $m = 4$. It is also worth mentioning that the anisotropic shift $\delta\sigma_{an}(H_4) = 18.3^A$, 18.8^B ppm in the complex $Au_3-(HF)_2^I$ is larger than that of water dimer (= 11.2 ppm).[18c]

A detailed comparison of the complexes $Au_3-(HF)_{2\le m\le 4}^I$ with the less stable ones, $Au_3-(HF)_{2\le m\le 4}^{II}$ (see Figures 1, 3, 5, and 7 and Table 1) leads us to postulate that the nonconventional hydrogen bond F−H···Au formed in the complexes $Au_3-(HF)_{2\le m\le 4}^I$ is the leading factor in their stabilization. Depending on the character of bonding, the $Au_3-(HF)_{2\le m\le 4}^{II}$ complexes can be partitioned into two classes. The complex $Au_3-(HF)_2^{II}$, stabilized by the nonconventional H-bond F−H···Au only (see Figure 3 and Table 1), belongs, by definition, to the first class. The other two, $Au_3-(HF)_3^{II}$ and $Au_3-(HF)_4^{II}$ (see Figures 5 and 7 and Table 1), formed solely by the anchor bond, are in the second class. The difference between these two classes comes from the number of HF molecules in the cluster: for the first class, we form a larger "ring" (the analogue of $(HF)_3$ or $(HF)_4$) with a better H-bonded geometry in the $(HF)_m$-part and two additional intermolecular bonds, whereas for the second class, we only slightly perturb the $(HF)_m$ ring and form only one still weaker intermolecular bond (see, e.g., ref 19 for the HF-rings with tails).

Let us consider the complex $Au_3-(HF)_2^{II}$. Its nonconventional hydrogen bonding is weaker than in $Au_3-(HF)_2^I$ since all the features essential in identifying H-bonds (viz., $\Delta R^I(F_3-H_4) - \Delta R^{II}(F_3-H_4) = 0.014-0.015$ Å, $\Delta\nu^I(F_3-H_4) - \Delta\nu^{II}(F_3-H_4) = -320$ to −296 cm^{-1}, and $r^I(H_4\cdots Au_6) - r^{II}(H_4\cdots Au_6) = -0.06$ Å) indicate a weaker character. This implies that the nonconventional hydrogen bonding interaction between Au_3 and $(HF)_2$ is strong enough to provide a stabilization of the complex alone, with a gain in energy of −4.9 to −4.8 kcal·mol^{-1}, hence leading to a lower-bound estimate to the H-bond formation energy $|E_{HB}| \ge 4.8-4.9$ kcal·mol^{-1}. This is the important feature showing that the anchor bonding is unable by itself to stabilize a complex between a triangle gold cluster Au_3 and $(HF)_2$. However, the anchor bond reinforces both the conventional and nonconventional hydrogen bondings. Figure 8 illustrates the above conclusion. It depicts the section of the PES of $Au_3-(HF)_2$ as a function of the anchoring F_1-Au_5 distance ranging from 2.0 to 3.7 Å. As $r(F_1\cdots Au_5)$ approaches 2.4 Å, the energy plot exhibits a minimum corresponding to the complex $Au_3-(HF)_2^I$. When the $r(F_1\cdots Au_5)$ further increases to 3.7 Å, the anchoring no longer holds, which results in a gradual decrease of the binding energy approximately to E_b-($Au_3-(HF)_2^{II}$) and a rather slow increase of the H-bond distance $r(H_4\cdots Au_6)$ within the range of 2.275−2.297 Å, that obviously obeys the van der Waals cutoff condition.

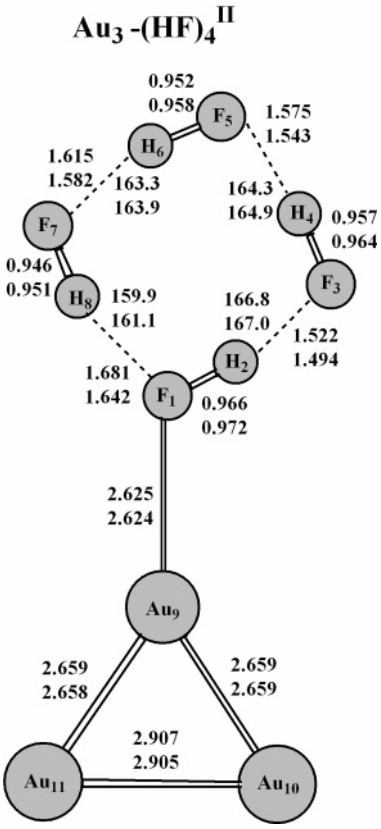

Figure 7. $Au_3-(HF)_4^{II}$ complex obtained within the B3LYP/RECP-(Au)∪A(H,F) (top entry) and B3LYP/RECP(Au)∪B(H,F) (lower entry) approaches. Its selected properties relevant for a further discussion are collected in Table 1. The bond lengths are given in Å and bond angles in deg. In addition, the values of some bond angles of $Au_3-(HF)_4^{II}$: $\angle H_2F_3H_4 = 106.6^{oA}$, 106.2^{oB}, $\angle H_4F_5H_6 = 106.5^{oA}$, 105.8^{oB}, $\angle H_6F_7H_8 = 107.4^{oA}$, 106.6^{oB}, $\angle H_8F_1H_2 = 105.2^{oA}$, 104.4^{oB}.

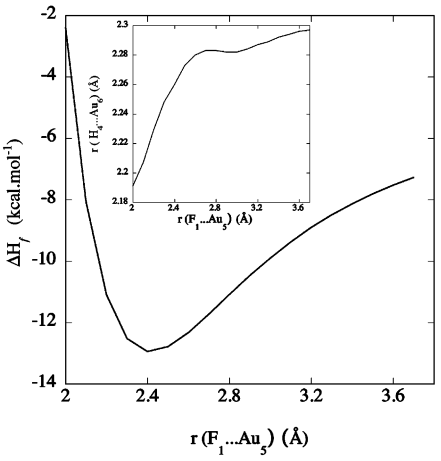

Figure 8. Section of the PES of $Au_3-(HF)_2$ as a function of $r(F_1\cdots Au_5) \in [2.0\ Å, 3.7\ Å]$ relative to the total energy of monomers. The insert depicts the optimized H-bond length $r(H_4\cdots Au_6)$ as a function of $r(F_1\cdots Au_5) \in [2.0\ Å, 3.7\ Å]$.

On the contrary, the complexes $Au_3-(HF)_{3\le m\le 4}^{II}$ that belong to the second class are solely stabilized by the anchor bonding. Because $(HF)_3$ and $(HF)_4$ remain therein cyclic, a F−H···Au nonconventional hydrogen bond cannot be formed, the anchoring is hence unbalanced and the complexes $Au_3-(HF)_3^{II}$ and $Au_3-(HF)_4^{II}$ are rather weakly bound: $E_b(Au_3-(HF)_3^{II}) = 2.8-2.9$ and $E_b(Au_3-(HF)_4^{II}) = 2.2-2.6$ kcal·mol^{-1}. They are even slightly weaker than Au_3-HF^I as indicated by the fact that the anchor bond in Au_3-HF^I is shorter by 0.01 and 0.05 Å than,

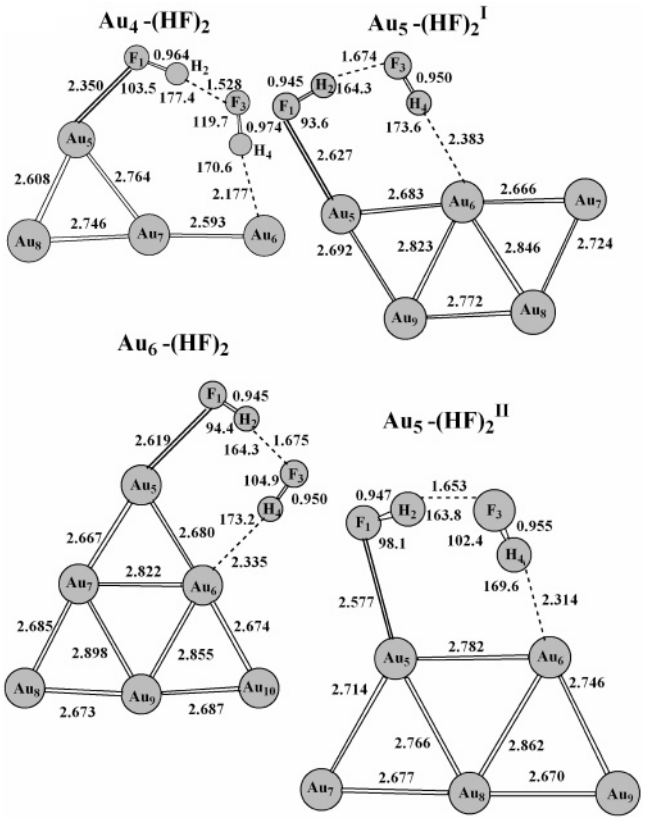

Figure 9. Most stable complexes $Au_{4\le n\le 6}-(HF)_2$ obtained within the B3LYP/RECP(Au)∪B(H,F) approach. The total dipole moment of the complex $Au_4-(HF)_2$ amounts to 2.32 D whereas it is slightly lower, 2.13 D, for $Au_6-(HF)_2$. The complexes $Au_5-(HF)_2^I$ and $Au_5-(HF)_2^{II}$ are less polar, 1.87 and 1.62 D, respectively. The H-bond $\nu_\sigma(F\cdots Au)$ stretch of these complexes $Au_4-(HF)_2$, $Au_5-(HF)_2^I$, $Au_5-(HF)_2^{II}$, and $Au_6-(HF)_2$ is equal to 138, 110, 110, and 110 cm^{-1}, respectively. The T-shape four-gold cluster $Au_4(C_{2v})$ has the following bond lengths: $r(Au_5-Au_7) = r(Au_7-Au_8) = 2.759$, $r(Au_5-Au_8) = 2.626$, and $r(Au_6-Au_7) = 2.573$ Å. Its electronic energy amounts to −543.921072 hartree,- its ZPVE = 0.788 kcal·mol^{-1}, and its enthalpy is equal to −543.911499 hartree. The properties of the most stable clusters $Au_{5\le n\le 7}$ are summarized in ref 16. The bond lengths are given in Å and bond angles in deg.

respectively, in $Au_3-(HF)_3^{II}$ and $Au_3-(HF)_4^{II}$. The anchoring bond is so weak in the latter complexes that it does not affect much the three-gold cluster, perturbing its bonds by only 0.003−0.01 Å.

Moreover, the H-bonded patterns in the HF rings of $Au_3-(HF)_3^{II}$ and $Au_3-(HF)_4^{II}$ are perturbed unfavorably compared to the isolated species. The reason is that their formation arises due to the anchoring bond that perturbs their $(HF)_m$ rings and destroys the C_{nh} symmetry of these rings. As a consequence, some of the hydrogen bonds which possess, within the isolated $(HF)_m$ ring, equal lengths become lengthened, whereas the others are shortened. The hydrogen bonds which are remote from the Au_3-"perturber" are almost unmodified. This pattern is indeed very similar to the HF-rings with tails.[19] Let us first consider the complex $Au_3-(HF)_3^{II}$. Since the Au_7-anchoring to F_1 lowers the proton donor ability of F_1, the F_1-H_2 bond is activated and lengthened by ∼ 0.01 Å compared to the isolated trimer $(HF)_3$. The neighboring F_3-H_4 bond remains unchanged. On the other side of the ring, because of the Au_7-F_1 anchoring, the F_1 atom repels the F_5-H_6 bond which is thus contracted by 0.007 Å. As a result, its stretching vibrational mode $\nu(F_5-H_6)$ undergoes a blue shift by ca. 170 cm^{-1}. Altogether, the contraction of the F_5-H_6 bond and the weakening of the proton acceptor−donor ability of F_1 due to its anchoring interaction with Au_7 entirely

TABLE 3: Selected Properties of the Most Stable Complexes $Au_{4\le n\le 7}-(HF)_2$ Obtained within the B3LYP/RECP(Au)∪B(H,F) Method[a]

complex	ΔR(F−H), Å	r(H···Au), Å	$\Delta\nu$(F−H), cm^{-1}	$\delta\sigma_{iso}$(H)
$Au_4-(HF)_2$ planar	$\Delta R(F_1-H_2)=0.032$	2.177	$-\Delta\nu(F_1-H_2)=588$	$\delta\sigma_{iso}(H_2)=-5.9$
	$\Delta R(F_3-H_4)=0.046$		$-\Delta\nu(F_3-H_4)=1023$	$\delta\sigma_{iso}(H_4)=-6.2$
			$A_{IR}(F_1-H_2\cdots F_3)/A_{IR}(F_1-H_2)=1.3$	
			$A_{IR}(F_3-H_4\cdots Au_6)/A_{IR}(F_3-H_4)=12.5$	
$Au_5-(HF)_2^{I}$ planar	$\Delta R(F_1-H_2)=0.013$	2.383	$-\Delta\nu(F_1-H_2)=250$	$\delta\sigma_{iso}(H_2)=-2.4$
	$\Delta R(F_3-H_4)=0.022$		$-\Delta\nu(F_3-H_4)=557$	$\delta\sigma_{iso}(H_4)=-2.9$
			$A_{IR}(F_1-H_2\cdots F_3)/A_{IR}(F_1-H_2)\approx 1.0$	
			$A_{IR}(F_3-H_4\cdots Au_6)/A_{IR}(F_3-H_4)=10.4$	
$Au_5-(HF)_2^{II}$ nonplanar $\angle F_3Au_6Au_8Au_5=35.3°$	$\Delta R(F_1-H_2)=0.015$	2.314	$-\Delta\nu(F_1-H_2)=286$	$\delta\sigma_{iso}(H_2)=-2.7$
	$\Delta R(F_3-H_4)=0.027$		$-\Delta\nu(F_3-H_4)=652$	$\delta\sigma_{iso}(H_4)=-3.1$
			$A_{IR}(F_1-H_2\cdots F_3)/A_{IR}(F_1-H_2)=1.2$	
			$A_{IR}(F_3-H_4\cdots Au_6)/A_{IR}(F_3-H_4)=12.0$	
$Au_6-(HF)_2$ planar	$\Delta R(F_1-H_2)=0.013$	2.335	$-\Delta\nu(F_1-H_2)=244$	$\delta\sigma_{iso}(H_2)=-2.4$
	$\Delta R(F_3-H_4)=0.022$		$-\Delta\nu(F_3-H_4)=549$	$\delta\sigma_{iso}(H_4)=-3.2$
			$A_{IR}(F_1-H_2\cdots F_3)/A_{IR}(F_1-H_2)=1.1$	
			$A_{IR}(F_3-H_4\cdots Au_6)/A_{IR}(F_3-H_4)=11.6$	
$Au_7-(HF)_2^{I}$ nonplanar $\angle F_3Au_6Au_9Au_7=163.2°$	$\Delta R(F_1-H_2)=0.016$	2.363	$-\Delta\nu(F_1-H_2)=290$	$\delta\sigma_{iso}(H_2)=-3.0$
	$\Delta R(F_3-H_4)=0.023$		$-\Delta\nu(F_3-H_4)=579$	$\delta\sigma_{iso}(H_4)=-3.3$
			$A_{IR}(F_1-H_2\cdots F_3)/A_{IR}(F_1-H_2)=0.9$	
			$A_{IR}(F_3-H_4\cdots Au_6)/A_{IR}(F_3-H_4)=10.0$	
$Au_7-(HF)_2^{II}$ planar	$\Delta R(F_1-H_2)=0.013$	2.398	$-\Delta\nu(F_1-H_2)=237$	$\delta\sigma_{iso}(H_2)=-2.3$
	$\Delta R(F_3-H_4)=0.020$		$-\Delta\nu(F_3-H_4)=484$	$\delta\sigma_{iso}(H_4)=-2.5$
			$A_{IR}(F_1-H_2\cdots F_3)/A_{IR}(F_1-H_2)=1.2$	
			$A_{IR}(F_3-H_4\cdots Au_6)/A_{IR}(F_3-H_4)=9.9$	
$Au_7-(HF)_2^{III}$ nonplanar $\angle F_3Au_5Au_{10}Au_6=34.7°$	$\Delta R(F_1-H_2)=0.014$	2.274	$-\Delta\nu(F_1-H_2)=269$	$\delta\sigma_{iso}(H_2)=-2.8$
	$\Delta R(F_3-H_4)=0.027$		$-\Delta\nu(F_3-H_4)=647$	$\delta\sigma_{iso}(H_4)=-3.5$
			$A_{IR}(F_1-H_2\cdots F_3)/A_{IR}(F_1-H_2)=1.2$	
			$A_{IR}(F_3-H_4\cdots Au_6)/A_{IR}(F_3-H_4)=13.9$	
$Au_7-(HF)_2^{IV}$ planar	$\Delta R(F_1-H_2)=0.012$	2.413	$-\Delta\nu(F_1-H_2)=212$	$\delta\sigma_{iso}(H_2)=-3.5$
	$\Delta R(F_3-H_4)=0.019$		$-\Delta\nu(F_3-H_4)=475$	$\delta\sigma_{iso}(H_4)=-0.8$
			$A_{IR}(F_1-H_2\cdots F_3)/A_{IR}(F_1-H_2)=1.2$	
			$A_{IR}(F_3-H_4\cdots Au_6)/A_{IR}(F_3-H_4)=10.3$	
$Au_7-(HF)_2^{V}$ nonplanar $\angle F_3Au_5Au_6Au_8=101.9°$	$\Delta R(F_1-H_2)=0.006$	2.352	$-\Delta\nu(F_1-H_2)=122$	$\delta\sigma_{iso}(H_2)=-1.0$
	$\Delta R(F_3-H_4)=0.018$		$-\Delta\nu(F_3-H_4)=439$	$\delta\sigma_{iso}(H_4)=-2.3$
			$A_{IR}(F_1-H_2\cdots F_3)/A_{IR}(F_1-H_2)=0.7$	
			$A_{IR}(F_3-H_4\cdots Au_6)/A_{IR}(F_3-H_4)=9.4$	

[a] The structures of these complexes are displayed in Figures 9−11. ΔR(F−H) is defined with respect to $(HF)_2$. $\Delta\nu$(F−H) is a shift of the stretching mode ν(F−H) taken relative to the corresponding monomer, and A_{IR} stands for its IR activity. $\delta\sigma_{Iso}$ (in ppm) is evaluated with respect to the corresponding monomers. It is worthwhile to mention that the complex $Au_7-(HF)_2^{III}$ is also formed via binding of the HF Dimer to the Au_6-Au_7 Bond of the 3D Complex Au_7^{II} (see Figure 3 in Ref 16B).

results in a considerable weakening of the H-contact $H_5\cdots F_1$ and causes its elongation by ca. 0.2 Å (see Figure 5). Similar changes occur in the H-bonded pattern of the complex $Au_3-(HF)_4^{II}$ (Figure 7) where the F_1-H_2 bond in the vicinity of the anchor bond Au_9-F_1 is elongated by 0.011 Å while the neighboring bond F_3-H_4 only by 0.003 Å. The other two, more distant bonds, F_5-H_6 and F_7-H_8, are correspondingly contracted by 0.002 and 0.008 Å. The $\nu(F_7-H_8)$ stretch exhibits a large blue shift of ca. 180 cm^{-1}.

The energy difference between $Au_3-(HF)_{3\le m\le 4}^{I}$ and $Au_3-(HF)_{3\le m\le 4}^{II}$ is rather large and reaches 10.7^{A}, 11.4^{B} kcal·mol^{-1} at $m=3$ and 7.1^{A}, 7.9^{B} kcal·mol^{-1} at $m=4$. These energy differences cover approximately 79−80% and 75−78% of the total binding energies of $Au_3-(HF)_3^{I}$ and $Au_3-(HF)_4^{I}$, respectively, thereby corroborating the above postulate of the leading role of the nonconventional hydrogen bonding in the stabilization of $Au_3-(HF)_3^{I}$ and $Au_3-(HF)_4^{I}$. One can therefore roughly estimate the energy E_{HB} of formation of the nonconventional hydrogen bond F−H···Au in the planar complexes $Au_3-(HF)_2^{I}$ and $Au_3-(HF)_3^{I}$ as equal to ca. −6 to −7 kcal·mol^{-1}. It is natural to end this Subsection by asking whether the ability to act as a nonconventional proton acceptor is a propensity of a three-gold cluster only or if larger clusters of gold are alike. This question is addressed in the next Subsection.

3.2. Potential Energy Surfaces of $Au_{4\le n\le 7}-(HF)_2$ Interaction. To answer the above question, let us consider Figures 9−11, where the most stable complexes $Au_{4\le n\le 7}-(HF)_2$ are shown, and Tables 1 and 3, where their relevant properties are gathered. First, we note that the $F_3-H_4\cdots Au_6$ bond, that is formed in all complexes $Au_{4\le n\le 7}-(HF)_2$ together with the anchor Au_5-F_1 bond (except the less stable complex $Au_7-(HF)_2^{V}$, stabilized only by the $F_3-H_4\cdots Au_6$ bond), satisfies all the conditions i−vi of the conventional hydrogen bonds (ref 11a; see also refs 1−9), viz., $\Delta R(F_3-H_4)=0.019-0.046$ Å (condition iii), r(H···Au) < 2.86 Å (van der Waals cutoff condition iv), $-\Delta\nu(F_3-H_4)=475-1023$ cm^{-1} (condition v), and the NMR chemical shift of the bridging proton $\delta\sigma_{iso}(H_4)=-0.8$ to −6.2 ppm (condition vi). The $F_3-H_4\cdots Au_6$ bond can therefore be treated as a nonconventional hydrogen bond of a moderate-strong type.

The strongest nonconventional hydrogen bond of the F−H···Au type within the entire series of the studied complexes $Au_{3\le n\le 7}-(HF)_{1\le m\le 4}$ is found in the complex $Au_4-(HF)_2$. As a working hypothesis, we suggest that its strongest character is mainly the result of two factors. The first and major factor is that the conventional donor group F_3-H_4 interacts with a singly coordinated gold atom, Au_6, that has a higher propensity to serve as a proton acceptor than the 2-fold coordinated gold atom in the complexes $Au_3-(HF)_{3\le m\le 4}^{I}$. As a result, the neighboring Au_6-Au_7 bond is weakened and elongates by 0.02 Å (see Figure 9). The second one is that the Au_5-F_1 anchoring bond is sufficiently strong (its length is equal to 2.350 Å; see Table 1)

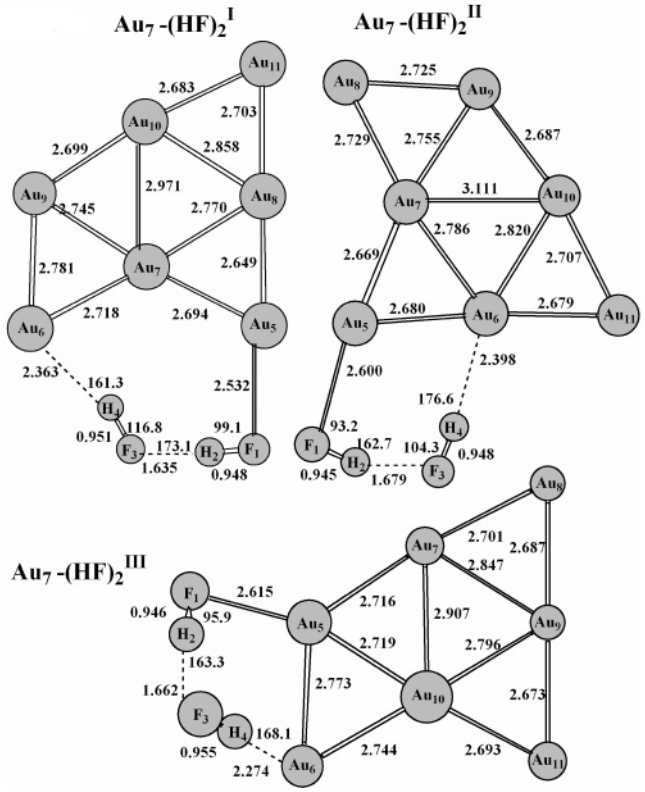

Figure 10. Most stable complexes $Au_7-(HF)_2^{I-III}$ obtained within the B3LYP/RECP(Au)∪B(H,F) approach. Their total dipole moments amount to 1.89, 1.60, and 2.24, respectively. Due a comparable entropy effect, $\Delta S = S(Au_7-(HF)_2^{I}) - S(Au_7-(HF)_2^{II}) \approx 2.7$ cal·mol^{-1}·T^{-1}, the Gibbs energy difference $\Delta G_{298} = G_{298}(Au_7-(HF)_2^{I}) - G_{298}(Au_7-(HF)_2^{II})$ amounts to -1.5 kcal·mol^{-1}. The bond lengths are given in Å and bond angles in deg.

to considerably affect the charge distribution: the differences in the Mulliken charges amount to $\Delta q(F_1) = -0.072$, $\Delta q(H_2) = 0.089$, $\Delta q(F_3) = -0.062$, $\Delta q(H_4) = -0.053$, $\Delta q(Au_5) = 0.211$, and $\Delta q(Au_6) = -0.016$ $|e|$ relative to those in the monomers. In view of the properties of this nonconventional hydrogen bond, primarily a large elongation of the F_3-H_4 bond by 0.046 Å and the significant red-shiftcomprising of 1023 cm^{-1}, we refer to it as a moderate-strong (ionic) nonconventional hydrogen bond.

Interestingly, the properties of the most stable complexes $Au_{3\le n\le 7}-(HF)_2$, gathered in Tables 1 and 3 and needed for proving that the F−H···Au bond formed therein shares all basic features with a conventional hydrogen bond, exhibit clear odd−even size oscillations. The latter are typical of neutral gold clusters (see ref 16a and references therein). In the present context, they indicate that even-size $Au_{2k}-(HF)_2$ complex possesses a more stable F−H···Au bond than the neighboring odd-size $Au_{2k-1}-(HF)_2$ one. Notice however that the above conjecture is obviously deduced from a limited number of complexes which are studied in the present work and might not therefore reflect a general trend. It is finally worth mentioning that, as follows from Tables 1 and 3, a less-coordinated gold atom (1 for $n = 3$, 4; 3 for $n = 5$; 4 for $n = 6$; and 2 for $n = 7$) better serves as a nonconventional proton acceptor to the donor F−H group of the HF dimer.

4. Summary

This work provides computational data that allow to unequivocally interpret the F−H···Au bonds, formed between small neutral clusters of gold and the hydrogen fluoride molecules, as nonconventional hydrogen ones. For all essential H-bonding features, the bonds of this type existing in the most stable complexes $Au_3-(HF)_{2\le m\le 4}^{I}$ are stronger than the O−H··· Au and N−H···Au bonds previously investigated.[11]

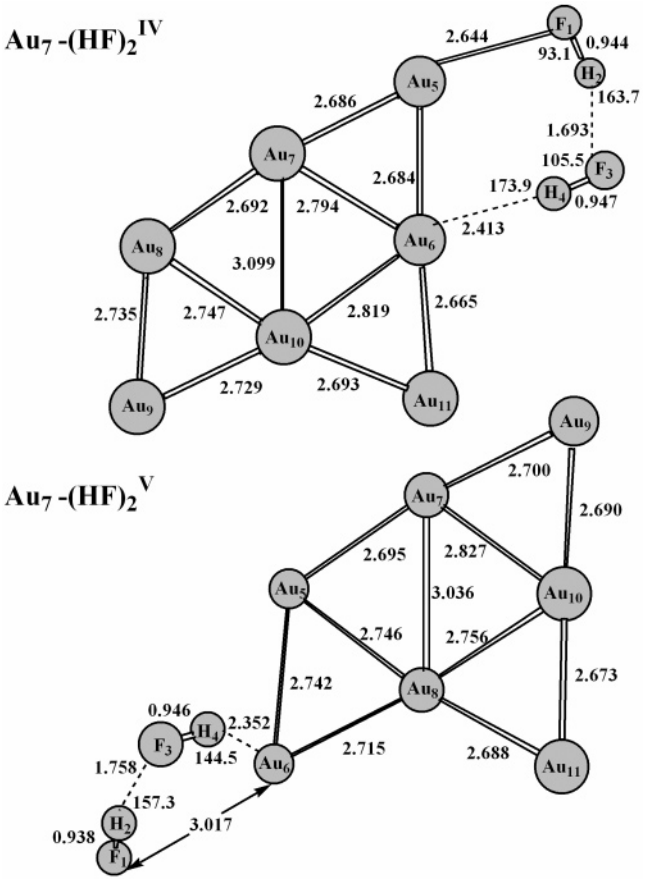

Figure 11. Most stable complexes $Au_7-(HF)_2^{IV-V}$ obtained within the B3LYP/RECP(Au)∪B(H,F) approach. Their total dipole moments are equal to 2.11 and 2.95 D, respectively. A comparable entropy effect is also predicted for the last two complexes, viz., $\Delta S = S(Au_7-(HF)_2^{V}) - S(Au_7-(HF)_2^{IV}) \approx 5.3$ cal·mol^{-1}·T^{-1}, that turns their Gibbs energy difference $\Delta G_{298} = G_{298}(Au_7-(HF)_2^{V}) - G_{298}(Au_7-(HF)_2^{IV})$ to the positive value of 0.9 kcal·mol^{-1}. The bond lengths are given in Å and bond angles in deg.

The mechanism of formation of the most stable complexes, $Au_{3\le n\le 7}-(HF)_{2\le m\le 4}$, relies on a cooperative interplay between the gold−halogen anchoring and the nonconventional hydrogen bonding where the latter often plays a key role. This drastically contrasts with the earlier studied systems[11] where the formation of either the Au−O or Au−N anchor bond is a crucial prerequisite for the O−H···Au and N−H···Au nonconventional H-bonding. In the most stable systems discussed here, covalent bonding, charge transfer, and electrostatic effects contribute to the Au−F anchoring and are mainly responsible for charge redistribution in both the gold and HF clusters subsystems. Within the gold cluster, the charge redistribution enhances the propensity of a given gold cluster to act as a nonconventional proton acceptor with the conventional proton donor. Within the HF cluster, it activates the neighboring F−H bond and, through the HF chain, intensifies backward the gold−halogen anchor bond. It is also inferred that the propensity of the unanchored Au atom to behave as a nonconventional proton acceptor is enhanced the less is its coordination number. This finding agrees with the recent conclusion by Freund and co-workers[20] that the chemical reactivity of gold nanoparticles originates from to the presence of lower-coordinated atoms of gold. It is precisely the case in the complex $Au_4-(HF)_2$ where the existence of a singly

coordinated Au atom in the T-shape Au_4 cluster promotes the formation of a strong nonconventional F−H···Au hydrogen bond. A strong character of this H-bond is reflected by a large red shift $\Delta\nu$(F−H) equal to 1023 cm^{-1} and by a large NMR isotropic shift $\delta\sigma_{iso}$ of the corresponding bridging proton of −6.2 ppm.

We anticipate that the estimates of the red shifts of the $\Delta\nu$-(F−H) stretching vibrational modes and of the energetics of the formation of the anchor and nonconventional F−H···Au hydrogen bondings determined above could be relevant for controlling the complexation of hydrogen fluoride clusters on gold particles. We also suggest that such nonconventional hydrogen bonding in the HF clusters adsorbed on gold surfaces could be characterized by IR spectroscopy, which therefore makes this bonding particularly useful as a recognition pattern in a surface catalysis involving gold particles.

Acknowledgment. This work was partially supported by Région Wallonne (Belgium, RW. 115012). The computational facilities were provided by NIC (University of Liège) and by F.R.F.C. 9.4545.03 and 1.5.187.05 (FNRS, Belgium). Parts of the calculations were performed on the Linux Cluster Schrödinger II at the University of Vienna. The authors are grateful for an ample supply of computer time on this installation. E.S.K. gratefully thanks Profs. Camille Sandorfy and George V. Yukhnevich for interesting discussions on the nonconventional A−H···Au hydrogen bonds, and F.R.F.C. 2.4562.03F (Belgium) for fellowship. We also thank the reviewer for valuable comments and suggestions.

References and Notes

(1) *Hydrogen Bonding*; Hadzi, D., Thompson, H. W., Eds.; Pergamon Press: London, 1959.

(2) Pimentel, C. G.; McClellan, A. L. *The Hydrogen Bond*; W. H. Freeman: San Francisco, 1960.

(3) *The Hydrogen Bond. Recent Developments in Theory and Experiments*, Schuster, P., Zundel, G., Sandorfy, C., Eds.; North-Holland: Amsterdam, 1976.

(4) Jeffrey, G. A.; Saenger, W. *Hydrogen Bonding in Biological Structures*; Springer: Berlin, 1991.

(5) Jeffrey, G. A. *An Introduction to Hydrogen Bonding*; Oxford University Press: Oxford, U.K., 1997.

(6) Scheiner, S. *Hydrogen Bonding. A Theoretical Perspective*; Oxford University Press: Oxford, U.K., 1997.

(7) Desiraju, G. R.; Steiner, T. *The Weak Hydrogen Bond in Structural Chemistry and Biology*; Oxford University Press: Oxford, U.K., 1999.

(8) Schuster, P. in *Intermolecular Interactions: From Diatomics to Biopolymers*; B. Pullman, B., Ed.; Wiley: Chichester, U.K., 1978; p 363.

(9) Steiner, T. *Angew. Chem. Int. Ed*. **2002**, *41*, 48.

(10) (a) Shubina, E. S.; Belkova, N. V.; Epstein, L. M. *J. Organomet. Chem*. **1997**, *17*, 536. (b) Orlova, G.; Scheiner, S. *Organometallics* **1998**, *17*, 4362. (c) Epstein, L. M.; Shubina, E. S. *Coord. Chem. Rev*. **2002**, *231*, 165 and references therein. (d) Brammer, L. *Dalton Trans*. **2003**, 3145 and references therein.

(11) (a) Kryachko, E. S.; Remacle, F. *Chem. Phys. Lett*. **2005**, *404*, 142. (b) Kryachko, E. S.; Remacle, F. *Nano Lett*. **2005**, *5*, 735.

(12) Karpfen, A. *Adv. Chem. Phys*. **2002**, *123*, 469.

(13) Frisch, M. J.; Trucks, G. W.; Schlegel, H. B.; Scuseria, G. E.; Robb, M. A.; Cheeseman, J. R.; Zakrzewski, V. G.; Montgomery, J. A.; Stratmann, R. E.; Burant, J. C.; Dapprich, S.; Millan, J. M.; Daniels, A. D.; Kudin, K. N.; Strain, M. C.; Farkas, O.; Tomasi, J.; Barone, V.; Cossi, M.; Cammi, R.; Mennucci, B.; Pomelli, C.; Adamo, C.; Clifford, S.; Ochterski, J.; Peterson, G. A.; Ayala, P. Y.; Cui, Q.; Morokuma, K.; Malick, D. K.; Rabuck, A. D.; Raghavachari, K.; Foresman, J. B.; Cioslowski, J.; Ortiz, J. V.; Stefanov, B. B.; Liu, G.; Liashenko, A.; Piskorz, P.; Komaromi, I.; Gomperts, R.; Martin, R. L.; Fox, D. J.; Keith, T.; Al-Laham, M. A.; Peng, C. Y.; Nanayakkara, A.; Gonzalez, C.; Challacombe, M.; Gill, P. M. W.; Johnson, B. G.; Chen, W.; Wong, M. W.; Andres, J. L.; Head-Gordon, M.; Replogle, E. S.; Pople, J. A. *GAUSSIAN 03*, Revision A.1; Gaussian, Inc.: Pittsburgh, PA, 2003.

(14) (a) Karpfen, A.; Kryachko, E. S. *J. Phys. Chem. A* **2003**, *107*, 9724. (b) Karpfen, A.; Kryachko, E. S. *Chem. Phys*. **2005**, *310*, 77.

(15) Ross, R. B.; Powers, J. M.; Atashroo, T.; Ermler, W. C.; LaJohn, L. A.; Christiansen, P. A. *J. Chem. Phys*. **1990**, *93*, 6654.

(16) (a) Remacle, F.; Kryachko, E. S. *Adv. Quantum Chem*. **2004**, *47*, 423. (b) Remacle, F.; Kryachko, E. S. *J. Chem. Phys*. **2005**, *122*, 044304.

(17) (a) Latajka, Z.; Scheiner, S. *Chem. Phys*. **1988**, *122*, 413. (b) Karpfen, A. *Int. J. Quantum Chem. Quantum Chem. Symp*. **1990**, *24*, 129. (c) Klopper, W.; Quack, M.; Suhm, M. A. *Mol. Phys*. **1998**, *94*, 105.

(18) (a) Hinton, J. F.; Wolinski, K. In *Theoretical Treatments of Hydrogen Bonding*, Hadzi, D., Ed.; Wiley: Chichester, U.K., 1997; p 75. (b) Becker, E. D. In *Encyclopedia of Nuclear Magnetic Resonance*; Grant, D. M., Harris, R. K., Eds.; Wiley: New York, 1996; p 2409. (c) Kar, T.; Scheiner, S. *J. Phys. Chem. A* **2004**, *108*, 9161 and references therein.

(19) Huisken, F.; Tarakanova, E. G.; Vigasin, A. A.; Yukhnevich, G. V. *Chem. Phys. Lett*. **1995**, *245*, 319.

(20) Lemire, C.; Meyer, R.; Shaikhutdinov, S.; Freund, H.-J. *Angew. Chem., Int. Ed*. **2004**, *43*, 118.